Anion-Exchange Equilibrium and Phase Segregation in Hydrotalcite Systems: Intercalation of Hexacyanoferrate(III) Ions

Matías Jobbágy[†] and Alberto E. Regazzoni*[,‡,§]

INQUIMAE, Facultad de Ciencias Exactas y Naturales, Universidad de Buenos Aires, Pabellón II, Ciudad Universitaria, 1428-Buenos Aires, Argentina, Unidad de Actividad Química, Centro Atómico Constituyentes, Comisión Nacional de Energía Atómica, Av. General Paz 1499, 1650-San Martín, Argentina, and Instituto de Tecnología Jorge A. Sábato, Universidad Nacional de General San Martín, Av. General Paz 1499, 1650-San Martín, Argentina

Received: August 31, 2004; In Final Form: October 21, 2004

The intercalation of hexacyanoferrate(III) in chloride-hydrotalcite was studied as a function of the composition of the equilibrated aqueous phase, the relevant solution variable being the ratio $(C_{Fe(CN)_6^{3-}})^{1/3}/C_{Cl^-}$. The isotherm shows that the exchange is markedly nonideal and reveals the segregation of two solid phases of fixed compositions at $(C_{Fe(CN)_6^{3-}})^{1/3}/C_{Cl^-} = 17.1\ M^{-2/3}$. This is the first case of solid phase segregation during anion exchange in hydrotalcite systems diagnosed from thermodynamic measurements. In agreement, PXRD patterns of the partially exchanged solids indicate that these phases, with distinct basal spacings, coexist in the range $0.21 \leq x \leq 0.86$. The observed behavior is accounted for by classical thermodynamic formalisms of ion exchange. The limitations of other representations commonly used to describe anion exchange in layered double hydroxide systems are stressed. A rationale of the structural changes accompanying the exchange is also offered.

Introduction

Layered double hydroxides (LDHs), the *negative* counterparts of clays, constitute a vast family of compounds of general formula $M(II)_{1-y}M(III)_y(OH)_2A_{y/z}\cdot nH_2O$, where y varies typically within 0.20 and 0.33. They are stacks of positively charged partially substituted brucite-like layers that are spaced by exchangeable A^{z-} anions and water molecules.[1]

The ability of LDHs to exchange interlamellar anions has been extensively exploited in the synthesis of a huge variety of intercalation compounds.[2,3] Due to their high maximum exchange capacity, they, as well as their memory-bearing calcined derivatives, are viewed as promising sorbents for the removal of anionic pollutants from aqueous systems.[4−6] Contrasting with the abundant literature referring to anion intercalation and properties of the intercalated materials, the dearth of thermodynamic information on anion-exchange equilibrium in LDHs systems is really surprising. Indeed, very few reports address equilibrated anion exchange,[7−11] and equilibrium constants are scanty; constants for pairs of simple symmetric exchanging anions can solely be found in the early work of Miyata[7] and the recent one by Israëli et al.[11] Studies on the energetics of anion exchange in LDHs are scarce as well.[11,12]

Aiming at contributing to the understanding of anion-exchange reactions involving LDHs, we present a thermodynamic and structural study of the intercalation of hexacyanoferrate(III) in chloride-hydrotalcite. The studied system was selected because hexacyanoferrate(III)-hydrotalcites are well characterized,[13−15] and because the possible contribution due to chemisorption at the particle edges, documented for selenate, arsenate, and phosphate,[16] can be safely ruled out.[17] Additionally, ferricyanide is common in various industrial effluents, and hydrotalcite-like minerals are frequent in nature.

Experimental Section

Hydrotalcite was prepared by coprecipitation.[1] 250 mL of a 0.5 M $AlCl_3$ and 1.0 M $MgCl_2$ solution was added dropwise, under vigorous stirring, to 100 mL of a 10^{-4} M NaOH solution, while the volume of 2 M NaOH required to keep pH 9 was dispensed from a pH-stat. The resulting suspension was then digested at 60 °C for 6 h. Then the solid was separated by centrifugation, washed thoroughly with water, and dried overnight under vacuum at 75 °C. The composition of the so-prepared solid, assessed by elemental analysis, was $Mg_{0.73}Al_{0.27}(OH)_2Cl_{0.19}(CO_3)_{0.04}\cdot H_2O$. Its PXRD pattern (Figure 1a) is typical of chloride-hydrotalcite. TEM showed that particles are ca. 0.1 μm size hexagonal platelets.

Anion-exchange experiments were performed in volumetric Pyrex flasks. A measured volume of a solution of known $K_3Fe(CN)_6$ and KCl concentrations was added to a weighted amount of a previously equilibrated suspension of hydrotalcite in water, and the volume of the flask completed with water. These suspensions were left to equilibrate at room temperature (23 ± 1 °C) for 1 h; equilibrium is attained within the first 20 min as indicated by preliminary experiments. They were filtered through 0.22 μm pore-size nitrocellulose membranes, and supernatants and filtrates were stored for analyses; filtrates were dried and kept in a desiccator. All experiments were carried out at pH 9.3 ± 0.1; i.e., the natural pH of hydrotalcite aqueous suspensions. For this purpose, the pH of all solutions was adjusted to 9.3 by addition of KOH. To avoid CO_3^{2-} contamination, all suspensions were kept under CO_2-free nitrogen.

The concentration of $Fe(CN)_6^{3-}$ in the supernatants was assessed photometrically ($\epsilon_{420} = 1015 \pm 2\ M^{-1}\ cm^{-1}$) in a

* Corresponding author. E-mail: regazzon@cnea.gov.ar.
[†] Universidad de Buenos Aires.
[‡] Comisión Nacional de Energía Atómica.
[§] Universidad Nacional de General San Martín.

10.1021/jp046063b CCC: $30.25
Published on Web 12/08/2004

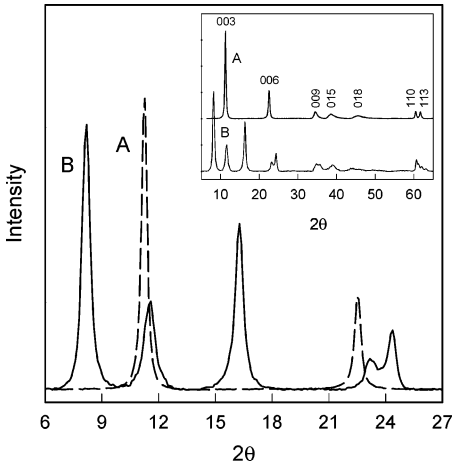

Figure 1. Detail of the $6° \leq 2\theta \leq 27°$ region of the PXRD diagrams of chloride-hydrotalcite (A) and ferricyanide-hydrotalcite (B). The inset shows the whole PXRD diagrams.

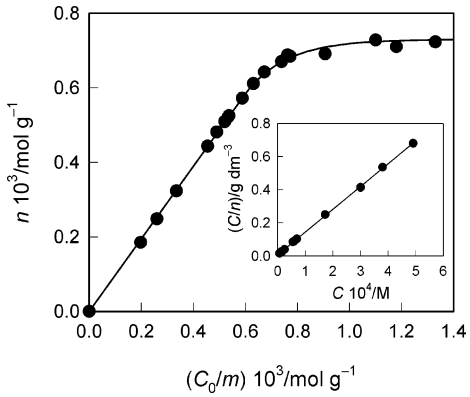

Figure 2. Exchanged hexacyanoferrate(III) as a function of the relative initial concentration; $m = 0.80$ g L^{-1}; no added KCl. Inset: Data replotted in the form of a linearized Langmuir adsorption isotherm (see eq 2).

Hewlett-Packard 8453 instrument using 1 cm, or 10 cm, optical-path quartz cells. The amount of exchanged $Fe(CN)_6^{3-}$ per gram of hydrotalcite (n) was determined from the difference between the initial (C_0) and the equilibrium ($C_{Fe(CN)_6^{3-}}$) concentrations. Since carbonate ions remained within the solid phase (see below) and pH did not change, the concentration of chloride ions in the equilibrated solution (C_{Cl^-}) was determined by solving the mass balance of the systems; preliminary potentiometric measurements carried out using a chloride-selective electrode substantiate this procedure.

In selected cases, the exchanged solids were characterized by powder X-ray diffraction and FTIR. PXRD patterns were recorded in a Siemens D-5000 diffractometer at 0.005° steps, 2 s counting time, using 0.1 mm slits, and the graphite-filtered Cu Kα radiation ($\lambda = 1.5406$ Å); peak analysis was performed using the Diffrac-AT 3.0 profile fitting software provided by the vendor. Transmission FTIR spectra were collected in a Nicolet Magna 560 instrument, after dispersing the samples in KBr.

Results and Discussion

Figure 2 shows the results of a series of experiments carried out at a fixed hydrotalcite load (m), increasing initial hexacyanoferrate(III) concentration, and no added KCl. They are presented in the form of an n vs C_0/m plot, which provides a simple manner of characterizing the exchange properties of LDHs.[18,19] At low relative initial concentrations, the amount of exchanged $Fe(CN)_6^{3-}$ increases linearly with C_0/m. The slope, 0.986, indicates that $Fe(CN)_6^{3-}$ ions are removed by the solid phase almost quantitatively. The slope decreases markedly at $C_0/m > 0.6$, and n levels off once $C_0/m \approx 1.15$. The value of n_{max} (7.3×10^{-4} mol g^{-1}) is in excellent agreement with the maximum exchange capacity that is derived from the solid stoichiometry (i.e., $Mg_{0.73}Al_{0.27}(OH)_2Cl_{0.19}(CO_3)_{0.04}\cdot H_2O$) and the stoichiometry of the exchange reaction (eq 1), provided interlamellar carbonate ions are assumed to be nonexchangeable.[4,5]

$$Fe(CN)_6^{3-}(aq) + 3\,Cl^-(ht) = 3\,Cl^-(aq) + Fe(CN)_6^{3-}(ht) \quad (1)$$

In eq 1, *ht* represents the exchanger solid phase.

Carbonate ions are in fact nonexchangeable, at least under the explored experimental conditions, as demonstrated by the PXRD patterns of hexacyanoferrate(III)-saturated hydrotalcite samples (Figure 1b). In addition to the peaks corresponding to the 003 (8.15°), 006 (16.28°), and 009 (24.34°) reflections of ferricyanide-hydrotalcite,[13,14] the patterns show peaks at 11.54° and 23.17°, which are due to the 003 and 006 reflections of carbonate-hydrotalcite.[20,21] Thus, the fully exchanged solid can be regarded as a mixture of $HT(Fe(CN)_6)_{1/3}$ and $HT(CO_3)_{1/2}$ (where HT stands for $[Mg_{2.7}Al(OH)_{7.4}\cdot nH_2O]^+$); interestingly, the relative area of the peaks at 8.15° and 11.54° that equals 2.36 matches the overall composition of the solid. This finding further suggests that the starting unexchanged solid may also be considered a mixture of HTCl and $HT(CO_3)_{1/2}$, although the latter phase cannot be detected (Figure 1a) because either the d_{003} spacings are too close to be clearly resolved (7.86 and 7.66 Å, respectively) or the interlamellar spaces occupied by CO_3^{2-} ions are randomly distributed within the hydrotalcite structure.

FTIR spectra of partially exchanged and hexacyanoferrate(III)-saturated hydrotalcites (Supporting Information) further confirm that $Fe(CN)_6^{3-}$ ions are unable to replace interlamellar carbonate; along with sharp bands at 2117 and 2034 cm^{-1} due to the $\nu_{C\equiv N}$ vibration of the intercalated complex,[15] all spectra depict the typical band of interlamellar free carbonate at ca. 1360 cm^{-1} (ref 22), which remains unaltered as the content of ferricyanide changes. The exceedingly large stability, thermodynamic and/or kinetic, of interlamellar carbonate ions has been traced back to its particular configuration (planar and parallel to the layers) that maximizes the electrostatic interactions between CO_3^{2-} and the brucite-like sheets.[23] Because under the present experimental conditions CO_3^{2-} ions are retained within the hydrotalcite structure, carbonate-filled interlamellar spaces shall hereafter be regarded as an innocent phase, its presence exerting no influence on the overall ferricyanide/chloride exchange behavior.

Results from experiments carried out at a fixed load of LDH and no added salt of the outgoing anion, such as those presented in Figure 2, have also been cast in terms of a linearized Langmuir adsorption isotherm,[8−10]

$$\frac{C_{Fe(CN)_6^{3-}}}{n} = \frac{1}{n_{max}K} + \frac{C_{Fe(CN)_6^{3-}}}{n_{max}} \quad (2)$$

This is however at variance with well-established thermodynamic formalisms,[24] because the equilibrium concentration of the outgoing anion varies throughout the data points. Compliance with eq 2 (see inset in Figure 2) is nonetheless fortuitous and stems from the insensitivity of this representation.

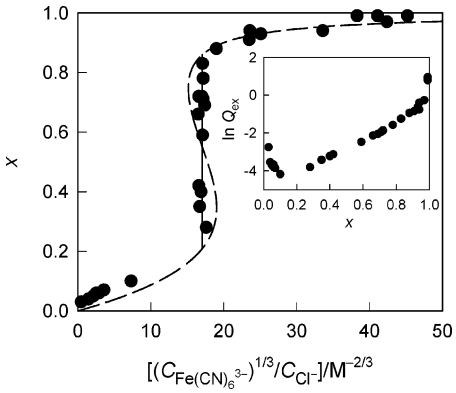

Figure 3. Hexacyanoferrate(III)/chloride exchange isotherm. The dashed line shows the prediction of eqs 5−7, and the solid line indicates the x range where the HTCl-rich and $HT(Fe(CN)_6)_{1/3}$-rich phases coexist (see text for details). Inset: ln Q_{ex} vs x.

Anion exchange involving LDHs can be described by either eq 1 or eq 3.

$$1/3\ Fe(CN)_6^{3-}(aq) + HTCl(s) = Cl^-(aq) + HT(Fe(CN)_6)_{1/3}(s) \quad (3)$$

Although these formalisms give different expressions for the exchange equilibrium constant, they are thermodynamically equivalent;[24] both describe the solid phase as a solid solution. Among them, we shall adopt the latter because it is simpler and offers a more rational description of the solid components (cf. eq 1). In this convention, the exchange equilibrium constant takes the form

$$K_{ex} = \frac{x\, f_{HT(Fe(CN)_6)_{1/3}}}{(1-x)\, f_{HTCl}} \frac{a_{Cl^-}}{(a_{Fe(CN)_6^{3-}})^{1/3}} \quad (4)$$

Thus, for dilute aqueous solutions, the equilibrium composition of the exchanger solid phase is simply given by

$$x = \frac{Q_{ex}(C_{Fe(CN)_6^{3-}})^{1/3}/C_{Cl^-}}{1 + Q_{ex}(C_{Fe(CN)_6^{3-}})^{1/3}/C_{Cl^-}} \quad (5)$$

where

$$Q_{ex} = K_{ex}(f_{HTCl}/f_{HT(Fe(CN)_6)_{1/3}}) \quad (6)$$

In these equations, x is the mole fraction of $HT(Fe(CN)_6)_{1/3}$, and $f_{HT(Fe(CN)_6)_{1/3}}$ and f_{HTCl} are the activity coefficients of the solid components.

Figure 3, which collects the results of all exchange experiments, presents x as a function of the relevant solution variable. As expected, all data points fall on the same curve, including those in which KCl was added to preequilibrated systems of fixed C_0/m; this latter finding indicates that the exchange process is reversible. Figure 3 shows that the exchange of chloride ions for hexacyanoferrate(III) in hydrotalcite is markedly nonideal. In addition, it reveals solid-phase segregation. The notorious independence of x with $(C_{Fe(CN)_6^{3-}})^{1/3}/C_{Cl^-}$ denotes the coexistence of two solid phases of fixed compositions; note that, at constant temperature and pressure, the variance of the system reduces from two to one. To our knowledge, this is the first case of phase segregation during anion exchange in LDH systems that has been diagnosed from solution measurements.

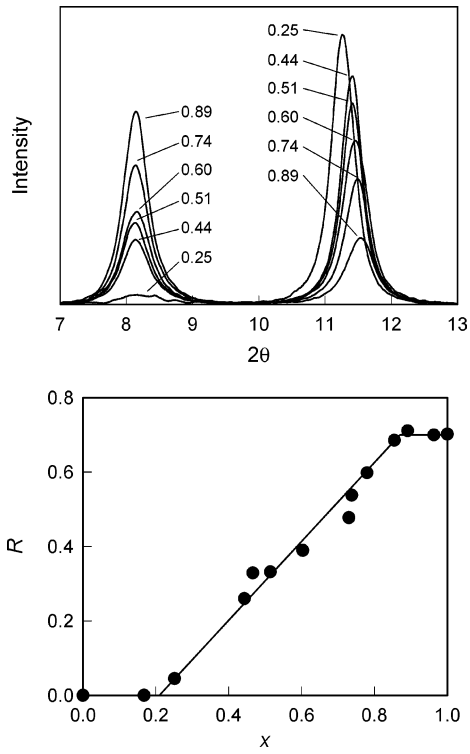

Figure 4. (A) Detail of the $7° \le 2\theta \le 13°$ region of the PXRD diagrams of partially exchanged hydrotalcites; x values are indicated by the labels; patterns have been smoothed for clarity. (B) Normalized relative area of the peak centered at 8.15° as a function of x.

Phase segregation is also demonstrated by the PXRD patterns of partially exchanged solids. Figure 4a, which shows the 2θ range where peaks due to the 003 reflections are located, indicates that the $HT(Fe(CN)_6)_{1/3}$-rich phase becomes distinguishable once x is about 0.25. It also shows that the position of the peak corresponding to the HTCl-rich phase shifts gradually, from 11.25° to 11.54° as the fraction of exchanged ferricyanide increases; the shift is arrested at $x \approx 0.85$. The evolution of the relative area of the peak due to the $HT(Fe(CN)_6)_{1/3}$-rich phase, i.e., $R = A_{8.15}/(A_{8.15} + A_{11.25-11.54})$, is presented in Figure 4b. These results indicate that $HT(Fe(CN)_6)_{1/3}$ forms at the expense of HTCl, only; viz., carbonate ions do not participate in the studied exchange reaction. In addition, Figure 4b shows that the $HT(Fe(CN)_6)_{1/3}$-rich and HTCl-rich phases coexist in the range $0.21 \le x \le 0.86$.

Phase segregation in partially exchanged naphthol-yellowS/Cl^-,[7] methyl-orange/Cl^-,[18] fluorescein/ClO_4^-,[19] and phosphate/Cl^-[25] LDH systems has already been documented by XRD. In other cases, second-staged phases, in which interlamellar spaces occupied by every anion are alternated along the c-axis, were detected.[26] In agreement with a previous XRD characterization of $HT(Fe(CN)_6)_{x/3}(NO_3)_{1-x}$ solids,[27] the patterns in Figure 4a do not evidence staging, which would be denoted by a peak at ca. 9.45° ($d = 9.35$ Å).

Since LDHs dispersed in water do not swell,[16a,26] we hypothesize that the first stages of hexacyanoferrate(III) intercalation involve the random displacement of the brucite-like sheets in the direction of the basal plane (see sketch in Figure 5). The disorder of the layers should increase as the exchange proceeds, until the galleries of this disrupted phase cannot accommodate further $Fe(CN)_6^{3-}$ ions. At this point ($x = x_\alpha = 0.21$), a new distinct solid whose basal spacing is determined by the size of the larger hexacyanoferrate(III) appears, the composition of the interlayer of this $HT(Fe(CN)_6)_{1/3}$-rich LDH ranging between $x_\beta = 0.86$ and 1. These ideas suggest that the

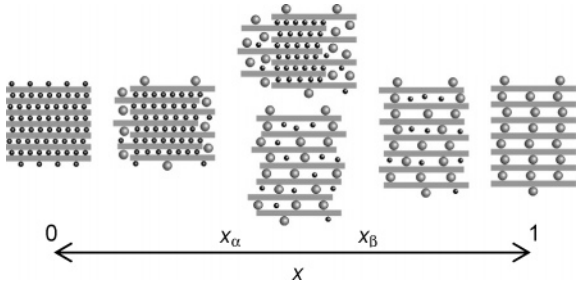

Figure 5. Structural changes accompanying the ferricyanide/chloride exchange in layered double hydroxides.

solubility of the larger incoming anion into the galleries of the disordered framework of brucite-like layers (i.e., the lower coexistence limit, x_α) should be influenced by the relative size of the exchanging anions. The available information is, however, insufficient to establish any possible correlation and does not allow for further analysis.

The structural changes accompanying anion exchange must reflect themselves on the concentration dependence of $f_{HT(Fe(CN)_6)_{1/3}}$ and f_{HTCl}. Modeling the different contributions to the excess Gibbs energy of mixing is indeed difficult, and due account of the nonideal behavior should require complex molecular calculations (see, e.g., ref 28). Nonetheless, the activity coefficients of the solid components can, in principle, be expressed in terms of the Margules expansion[24] or the equivalent Redlich−Kister expression (eq 7).[29]

$$RT\ln\frac{f_{HT(Fe(CN)_6)_{1/3}}}{f_{HTCl}} = a(1-2x) + b(1-6x+6x^2) + \cdots \quad (7)$$

where a and b are constant parameters, the latter accounting for the noted asymmetry with respect to $x = 0.5$. The line in Figure 3 indicates that, under the constraint impose by the coexistence of the HTCl-rich and $HT(Fe(CN)_6)_{1/3}$-rich phases, eq 5, together with eqs 6 and 7, is a good descriptor of the observed exchange behavior. For the coexistence limits derived from Figure 4b, $K_{ex} = 0.0617\ M^{2/3}$, $a/RT = 2.377$, and $b/RT = -0.1834$ (see Appendix). The fitting of the data can be improved if further terms are included in eq 7. The value of K_{ex} is in good agreement with that calculated using eq 8 and the Kielland plot shown in the inset of Figure 3. This procedure, customarily used in the literature,[7,11] is however silent toward solid-phase segregation.[30] The difference, $\Delta = -0.24$ (see the original treatment of Gaines and Thomas[31]), suggests that changes in interlayer hydration are nonnull for asymmetric anion-exchange reactions involving LDHs (cf. ref 7).

$$\ln K_{ex} = \int_0^1 \ln Q_{ex}\, dx \quad (8)$$

K_{ex} embodies different contributions to the standard Gibbs energy of anion exchange. Among them, the most important are changes in the electrostatic interaction between the brucite-like sheets and the intercalated anions, and changes in anion solvation.[32] A comparison with Miyata's data[7] suggests, however, that for asymmetric anion-exchange processes changes in the electrostatic repulsion between the intercalated anions may also be of importance; the hexacyanoferrate(III)/Cl^- exchange constant is much lower than predicted from z/r considerations. The role of anion−anion repulsive interactions has been nicely illustrated by Xu and Zeng,[33] who showed that interlamellar nitrate ions change their orientation as the charge density of the brucite-like sheets, hence the nitrate density, is increased, producing an expansion of the basal spacing at a given y value.

For organic anions, the ease of the intercalation process indicates that anion configuration, and dispersive interactions between the guest anions,[34] as well as hydrogen bonding for amino acids,[12] are also factors that influence anion selectivities. Clearly, molecular modeling shall help assess the various contributions to ΔG°_{ex}.

The recent thermochemical approach proposed by Allada et al.[35] to compute the Gibbs energy of formation of LDHs can, in principle, be used to estimate K_{ex}. The approach relies on the mechanical mixture approximation, which allows $\Delta_f G^\circ_{LDH}$ to be assessed from $\Delta_f G^\circ$ values of the individual hydroxides and $M(II)_zA_2$ salts. The lack of data for magnesium ferricyanide precludes, however, any possible estimation. Interestingly, the approach predicts reasonably well the trend depicted by the data of Miyata[7] and Israëli et al.,[11] although it overestimates the reported exchange constants. A thorough analysis of the predicting capabilities of Allada's and other thermochemical models can be found in the very recent publications by Bravo-Suárez et al.[36]

Undoubtedly, the design of water treatment procedures based on the exchange ability of LDHs requires appropriate thermodynamic descriptions, which are in fact furnished by classical formalisms. In addition, they provide a way of accounting for the marked departure from ideality that eventually reflects itself as solid phase segregation. Incidentally, this nonideal behavior should affect greatly the solubility of LDHs in water (which depends on the overall composition of the interlayer[35]), a fact that may have important implications on the composition of natural aquifers.

It is worth stressing that although the use of LDHs for removing anionic contaminants seems auspicious, a detailed characterization of equilibrated anion exchange in the many systems of interest is still lacking.

Acknowledgment. This work is part of CNEA's P5-PID-36-1. Support from ANPCyT (PICT 06-06631) is gratefully acknowledged. A.E.R. is member of CONICET. M.J. is a Gabbo's fellow. We are indebted to M. L. Japas for helpful discussions.

Supporting Information Available: FTIR spectra of unexchanged, partially exchanged and hexacyanoferrate(III)-saturated hydrotalcites (PDF). This material is available free of charge via the Internet at http://pubs.acs.org.

Appendix

Parameters a and b of the Redlich−Kister expression (eq 7) were determined from the values of the mole fraction of $HT(Fe(CN)_6)_{1/3}$ that correspond to the limits of the coexistence region. Briefly, coexistence implies that

$$\Delta\mu_B^{\alpha} - \Delta\mu_A^{\alpha} = \Delta\mu_B^{\beta} - \Delta\mu_A^{\beta} \quad (A.1)$$

$$\Delta\mu_B^{\alpha} = \Delta\mu_B^{\beta} \quad (A.2)$$

where A and B represent HTCl and $HT(Fe(CN)_6)_{1/3}$, and α and β denote the HTCl-rich and $HT(Fe(CN)_6)_{1/3}$-rich phases, respectively. $\Delta\mu_i$ is the difference between the chemical potential of component i and the respective Raoult reference state. From basic thermodynamics,[29]

$$\Delta\mu_B - \Delta\mu_A = (\partial\Delta G_{mix}/\partial x)_{P,T} \quad (A.3)$$

$$\Delta\mu_B = \Delta G_{mix} + (1-x)(\partial\Delta G_{mix}/\partial x)_{P,T} \quad (A.4)$$

and the Gibbs energy of mixing being given by

$$\Delta G_{mix} = \Delta G_{id} + a(x - x^2) + b(x - x^2)(1-2x) \quad (A.5)$$

Thus, eqs A.1 and A.2 can be rewritten as

$$a2(x_\alpha - x_\beta) + b[6(x_\alpha - x_\beta) - 6({x_\alpha}^2 - {x_\beta}^2)] + \ln\frac{x_\beta(1 - x_\alpha)}{x_\alpha(1 - x_\beta)} = 0 \quad (A.6)$$

$$a[2(x_\alpha - x_\beta) - ({x_\alpha}^2 - {x_\beta}^2)] + b[6(x_\alpha - x_\beta) - 9({x_\alpha}^2 - {x_\beta}^2) + 4({x_\alpha}^3 - {x_\beta}^3)] + \ln\frac{x_\beta}{x_\alpha} = 0 \quad (A.7)$$

which yield a and b, provided x_α and x_β are known; the latter are the lower and upper limits of the coexistence region, respectively.

Finally, the value of K_{ex} was calculated from

$$K_{ex} = g \exp[({\Delta\mu_B}^\alpha - {\Delta\mu_A}^\alpha)/RT] \quad (A.8)$$

where g is the reciprocal of the value taken by the relevant solution variable at the coexistence line.

References and Notes

(1) Cavani, F.; Trifirò, F.; Vaccari, A. *Catal. Today* **1991**, *11*, 173.
(2) Rives, V.; Ulibarri, M. A. *Coord. Chem. Rev.* **1999**, *181*, 61.
(3) Khan, A. I.; O'Hare, D. *J. Mater. Chem.* **2002**, *12*, 3191.
(4) Sato, T.; Wakabayashi, T.; Shimada, M. *Ind. Eng. Chem. Prod. Res. Dev.* **1986**, *25*, 89.
(5) Parker, L. M.; Milestone, N. B.; Newman, R. H. *Ind. Eng. Chem. Res.* **1995**, *34*, 1196.
(6) (a) Houri, B.; Legrouri, A.; Barroug, A.; Forano, C.; Besse, J.-P. *J. Chim. Phys.* **1999**, *96*, 455. (b) Lakraimi, M.; Legrouri, A.; Barroug, A.; de Roy, A.; Besse, J.-P. *J. Chim. Phys.* **1999**, *96*, 470. (c) Lazaridis, N. K.; Hourzemanoglou, A.; Matis, K. A. *Chemosphere* **2002**, *47*, 319. (d) Lazaridis, N. K.; Pandi, T. A.; Matis, K. A. *Ind. Eng. Chem. Res.* **2004**, *43*, 2209.
(7) Miyata, S. *Clay Clays Miner*. **1983**, *31*, 305.
(8) Ookubo, A.; Ooi, K.; Hayashi, H. *Langmuir* **1993**, *9*, 1418.
(9) Hermosín, M. C.; Pavlovic, I.; Ulibarri, M. A.; Cornejo, J. *Water Res.* **1996**, *30*, 171.
(10) Das, J.; Das, D.; Dash, G. P.; Parida, K. M. *J. Colloid Interface Sci.* **2002**, *251*, 26.
(11) Israëli, Y.; Taviot-Guého, C.; Besse, J.-P.; Morel, J.-P.; Morel-Desrosiers, N. *Dalton* **2000**, 791.
(12) Morel-Desrosiers, N.; Pisson, J.; Israëli, Y.; Taviot-Guého, C.; Besse, J.-P.; Morel, J.-P. *J. Mater. Chem.* **2003**, *13*, 2582.
(13) Idemura, S.; Susuki, E.; Ono, Y. *Clay Clays Miner*. **1989**, *6*, 553.
(14) Holgado, M. J.; Rives, V.; Sanromán, M. S.; Malet, P. *Solid State Ionics* **1996**, *92*, 273.
(15) Kloprogge, J. T.; Weier, M.; Crespo, I.; Ulibarri, M. A.; Barriga, C.; Rives, V.; Martens, W. N.; Frost, R. L. *J. Solid State Chem.* **2004**, *177*, 1382.
(16) (a) Hou, X.; Kirkpatrick, R. J. *Chem. Mater.* **2000**, *12*, 1890. (b) Randall, S. R.; Sherman, D. M.; Vala-Ragnarsdottir, K. *Geochim. Cosmochim. Acta* **2001**, *65*, 1015. (c) Jobbágy, M. Ph.D. Thesis, Universidad de Buenos Aires, Argentina, 2003.
(17) (a) Huang, C.; Cheng, W. P. *J. Colloid Interface Sci.* **1997**, *188*, 270. (b) Cheng, W. P.; Huang, C.; Pan, J. R. *J. Colloid Interface Sci.* **1999**, *204*, 213.
(18) Costantino, U.; Coletti, N.; Nocchetti, M.; Aloisi, G. G.; Elisei, F. *Langmuir* **1999**, *15*, 4454.
(19) Costantino, U.; Coletti, N.; Nocchetti, M.; Aloisi, G. G.; Elisei, F.; Latterini, L. *Langmuir* **2000**, *16*, 10351.
(20) Miyata, S. *Clay Clays Miner*. **1980**, *28*, 50.
(21) Belloto, M.; Rebours, B.; Clause, O.; Lynch, J.; Bazin, D.; Elkaïm, E. *J. Phys. Chem.* **1996**, *100*, 8527.
(22) Labajos, F. M.; Rives, V. *Inorg. Chem.* **1996**, *35*, 5313.
(23) Xu, Z. P.; Zeng, H. C. *Chem. Mater.* **2001**, *13*, 4555.
(24) Sposito, G. *The Thermodynamics of Soil Solutions*; Oxford Science Publ.: Oxford, 1981.
(25) Ookubo, A.; Ooi, K.; Tani, F.; Hayashi, H. *Langmuir* **1994**, *10*, 407.
(26) (a) Fogg, A. M.; Dunn, J. S.; O'Hare, D. *Chem. Mater.* **1998**, *10*, 356. (b) Pisson, J.; Taviot-Guého, C.; Israëli, Y.; Leroux, F.; Munsch, P.; Itié, J.-P.; Briois, V.; Morel-Desrosiers, N.; Besse, J.-P. *J. Phys. Chem. B* **2003**, *107*, 9243.
(27) Nijs, H.; De Bock, M.; Vansant, E. F. *Microporous Mesoporous Mater.* **1999**, *30*, 243.
(28) (a) Aicken, A. M.; Bell, I. S.; Coveney, P. V.; Jones, W. *Adv. Mater.* **1997**, *9*, 496. (b) Fogg, A. M.; Rohl, A. L.; Parkinson, G. M.; O'Hare, D. *Chem. Mater.* **1999**, *11*, 1194. (c) Wang, J.; Kalinichev, A. G.; Kirkpatrick, R. J.; Hou, X. *Chem. Mater.* **2001**, *13*, 145.
(29) Prausnitz, J. M.; Lichtenthaler, R. N.; Gomes de Azevedo, E. *Molecular Thermodynamics of Fluid-Phase Equilibria*, 3rd ed.; Prentice Hall: London, 1999.
(30) Barrer, R. M.; Klinowski, J. *J. Chem. Soc., Faraday Trans. 1* **1972**, *68*, 73.
(31) Gaines, G. L.; Thomas, H. C. *J. Chem. Phys.* **1953**, *21*, 714.
(32) Dutta, P. K.; Puri, M. *J. Phys. Chem.* **1989**, *93*, 376.
(33) Xu, Z. P.; Zeng, H. C. *J. Phys. Chem. B* **2001**, *105*, 1743.
(34) (a) Tagaya, H.; Sato, S.; Morioka, H.; Kadokawa, J.-I.; Karasu, M.; Chiba, K. *Chem. Mater.* **1993**, *5*, 1431. (b) Fogg, A. M.; Dunn, J. S.; Shyu, S.−G.; Cary, D. R.; O'Hare, D. *Chem. Mater.* **1998**, *10*, 351; (c) Lei, L.; Millange, F.; Walton, R. I.; O'Hare, D. *J. Mater. Chem.* **2000**, *10*, 1881. (d) Lei, L.; Vijayan, R. P.; O'Hare, D. *J. Mater. Chem.* **2001**, *11*, 3276.
(35) Allada, R. K.; Navrotski, A.; Thompson-Berbeco, H.; Casey, W. H. *Science* **2002**, *296*, 721.
(36) (a) Bravo-Suárez, J. J.; Páez-Mozo, E. A.; Oyama, S. T. *Quim. Nova* **2004**, *27*, 574. (b) Bravo-Suárez, J. J.; Páez-Mozo, E. A.; Oyama, S. T. *Quim. Nova* **2004**, *27*, 601.